

SUPPLEMENTARY INFORMATION**Pregnenolone Sulphate- and Cholesterol-Regulated TRPM3 Channels
Coupled to Vascular Smooth Muscle Secretion and Contraction**

Jacqueline Naylor¹⁻³, Jing Li¹⁻³, Carol J Milligan¹⁻³, Fanning Zeng¹⁻³, Piruthivi Sukumar¹⁻³, Bing Hou¹⁻³, Alicia Sedo¹⁻³, Nadira Yuldasheva^{1,4}, Yasser Majeed¹⁻³, Dhananjay Beri¹⁻³, Shan Jiang¹⁻³, Victoria AL Seymour¹⁻³, Lynn McKeown¹⁻³, Bhaskar Kumar^{2,3}, Christian Harteneck⁵, David O'Regan⁶, Stephen B Wheatcroft^{1,4}, Mark T Kearney^{1,4}, Clare Jones⁷, Karen E Porter^{1,4} & David J Beech^{1-3*}

¹Multidisciplinary Cardiovascular Research Centre and ²Institute of Membrane & Systems Biology, Faculties of ³Biological Sciences and ⁴Medicine & Health, University of Leeds, Leeds, LS2 9JT, UK. ⁵Institute of Pharmacology and Toxicology, Eberhard-Karls-University, Wilhelmstr. 56, 72074 Tübingen, Germany. ⁶Department of Cardiac Surgery, Leeds General Infirmary, Great George Street, Leeds, LS1 3EX. ⁷Respiratory & Inflammation AstraZeneca R&D Charnwood, Bakewell Road, Loughborough, Leicestershire LE11 5RH, UK.

*author for correspondence: Professor David J Beech, Institute of Membrane & Systems Biology, Garstang Building, Faculty of Biological Sciences, University of Leeds, Leeds, LS2 9JT, England (UK). Tel: +44-(0)-113-343-4323; Fax: +44-(0)-113-343-4228; Email: d.j.beech@leeds.ac.uk

Detailed Methods**Human vein and cell culture**

Freshly discarded human saphenous vein segments were obtained anonymously and with informed consent from patients undergoing open heart surgery in the General Infirmary at Leeds. Approval was granted by the Leeds Teaching Hospitals Local Research Ethics Committee. Proliferating vascular smooth muscle cells (VSMCs) were prepared using an explant technique and grown in Dulbecco's Modified Eagle's Medium (DMEM) supplemented with 10 % foetal calf serum (FCS), penicillin/streptomycin and L-glutamine at 37 °C in a 5 % CO₂ incubator. Experiments were performed on cells passaged 2-5 times. VSMCs stained positively for smooth muscle α -actin. For culture of endothelial cells (ECs), endothelium was digested using 1 mg/ml Type II collagenase (Worthington Biochemicals, UK) dissolved in Medium 199 (Sigma, UK) (37 °C, 15 min). Cells were resuspended in M199 supplemented with 20 % FCS and 1 % penicillin-streptomycin and including endothelial growth factor (15 μ g/ml) and pyruvate (1 μ M). Cells were used up to passage 3. Growth of neointima has been described¹. HEK 293 cells were maintained in Dulbecco's Modified Eagle's Medium (DMEM)-F12 + Glutamax-1 (Gibco) supplemented with 10 % FCS and penicillin-streptomycin at 37 °C in a 5 % CO₂ incubator.

Mouse femoral artery injury

12 week old male C57/BL6 mice were anaesthetized and the left femoral arteries were isolated under aseptic conditions. A small area of the femoral artery was partially transected to allow the passage of a guide wire into the vessel. The guide wire was then removed and the incision closed. A sham procedure (without guide wire passage) was performed on the opposite leg for comparison. At 21 days post injury, mice were anaesthetized and perfused with 4 % paraformaldehyde. Procedures were conducted in accord with accepted standards of humane animal care under UK Home Office Project License 40/2988. Femoral artery bundles were removed and embedded in paraffin wax. For histological staining, sections 10 μ m thick were mounted onto slides.

Physiological mouse aorta

Eight week old male C57/BL6 mice were killed by CO₂ asphyxiation and cervical dissociation in accordance with Schedule 1 Code of Practice, UK Animals Scientific Procedures Act 1986. The thoracic

aorta was removed and placed in ice-cold Hanks solution. Fat was removed completely by dissection and blood was flushed from the lumen with Hanks solution. Hanks solution contained (mmole/L): NaCl, 137; KCl, 5.4; CaCl₂, 0.01; NaH₂PO₄, 0.34; K₂HPO₄, 0.44; D-glucose, 8; Hepes, 5.

RNA isolation and RT-PCR

Total RNA was extracted using a Tri-reagent protocol followed by DNase I (Ambion) treatment. 1 µg of total RNA was used for reverse transcription (RT) based on oligo-dT primers and AMV RT enzyme. The specificity of PCR was verified by reactions without RT (-RT) and by melt-curve analysis of PCR products. PCR products were electrophoresed on 2 % agarose gels containing ethidium bromide. Sequences of PCR primers are in Supplementary Table I. PCR products were sequenced to confirm identity (Leeds University Sequencing Facility or Lark UK).

Quantitative RT-PCR

Quantitative, real-time, PCR was carried out using a Lightcycler (Roche). Relative abundance of target RNA was normalized to β-actin RNA, which showed no difference between samples. PCR efficiency (E) was $10^{-(1/\text{slope})}$. Relative abundance of target RNA was calculated from $(E_{\beta\text{-actin}}^{C_p}) / (E_{\text{target}}^{C_p})$, where PCR cycle crossing-points (C_p) were determined by fit-points methodology.

TRPM3 cDNA expression

Human TRPM3 cDNA (accession number AJ505026) was used for over-expression studies². For most experiments we used stable expression of the human TRPM3 in the T-REx expression system (Invitrogen, UK), as previously described². The T-REx cells were maintained in the presence of 400 µg/mL zeocin and 5 µg/mL blasticidin S (InvivoGen). To induce TRPM3 expression cells were incubated with 1 µg/mL tetracycline (Sigma, UK) for 24-72 hr prior to experiments. Non-induced cells without addition of tetracycline (Tet-) were used as controls. In some experiments, where specified, we used transient transfection for TRPM3 expression²: Briefly, wild-type HEK 293 cells were plated onto poly-L-lysine coated coverslips and grown to ~80 % confluency. 1 µg TRPM3-YFP or YFP cDNA was transfected into the cells using FuGENE 6 (Roche, UK). Functional studies were carried out 48 hr after transfection on YFP-fluorescent cells. Also in a small number of experiments we used mouse TRPM3α2 cDNA (accession number AJ544535) in pCAGGSM2-IRESGFP was a gift from Dr SE Philipp³. 1 µg TRPM3α2 was co-transfected into HEK 293 cells with GFP using FuGENE 6 (Roche, UK). Functional studies were carried out 48 hr after transfection on GFP-fluorescent cells.

Transfection with siRNA

0.5-2 x10⁶ VSMCs were centrifuged (100 g) for 10 min, resuspended in Basic Nucleofector solution (Amaxa GmbH, Germany), mixed with 1 µmole/L short interfering (si) RNA and transferred into a cuvette for electroporation (Amaxa). The scrambled control siRNA was Silencer Negative Control #1, a 19 bp scrambled sequence with no significant homology to human gene sequences (Ambion Europe Ltd). Cells were transferred from cuvettes to pre-warmed culture medium and incubated in a 5 % CO₂ incubator at 37 °C. Culture medium was changed after 24 hr and recordings were made after a further 24 hr. Transfection efficiency was about 80 %. TRPM3 siRNA was (sense strand, 5'-3') CCCAAUGUGAUCUCGAUUGtt (Ambion). Smart pool TRPM3 siRNA-2 was a mixture of GAGAUGUUGUCCGGCCAU, GAAGGAUCAUGCCUCUAAG, GACCCAAUGUGAUCUCGAU and GAGCGUGGAUUAUCACUGG (Dharmacon).

Intracellular Ca²⁺ measurement

Cells were pre-incubated with fura-2AM for 1 hr at 37 °C followed by a 0.5 hr wash at room temperature (21±2 °C). Measurements were made at room temperature on a fluorescence microscope (Zeiss, Germany) or a 96-well fluorescence plate reader (FlexStation II³⁸⁴, Molecular Devices). The inverted microscope was equipped with a 40x Fluor oil-immersion objective (NA 1.3). Fura-2 dye was excited by light of 340 and 380 nm from a xenon arc lamp, the wavelength of which was selected by a

monochromator (Till photonics, Germany). Emitted light at 510 nm was collected via an emission filter and images captured every 10 s by an Orca-ER digital camera (Hamamatsu, Japan). The same excitation wavelengths were used in the FlexStation, where wells within columns of the 96-well plate were loaded alternately for test and control conditions. For either method, the intracellular calcium (Ca^{2+}) concentration is indicated as the ratio of fura-2 fluorescence (F) emission intensities for 340 nm and 380 nm excitation. The recording solution (standard bath solution, SBS) contained (mmole/L): 130 NaCl, 5 KCl, 8 D-glucose, 10 HEPES, 1.5 CaCl_2 and 1.2 MgCl_2 , titrated to pH 7.4 with NaOH. When 0 Ca^{2+} is indicated, CaCl_2 was omitted and replaced by 0.4 mmole/L EGTA.

Chemical screen

Cells were pre-incubated with fluo3 AM for 1 hr at 37 °C followed by a wash at room temperature (21 ± 2 °C). Measurements were made at room temperature on a 96-well fluorescence plate reader (FLIPR, Molecular Devices). Fluo3 dye was excited by light of 485 nm, and emitted light collected at 525 nm. Wells within columns of the 96-well plate were loaded alternately for test and control conditions. The recording solution (standard bath solution, SBS) contained (mmole/L): 130 NaCl, 5 KCl, 8 D-glucose, 10 HEPES, 1.5 CaCl_2 and 1.2 MgCl_2 , titrated to pH 7.4 with NaOH. Response amplitudes were graded to a colour scale, with 1 being the maximal response (dark green) and a lack of response < 0.1 (white).

Cholesterol delivery

Cells were pre-treated with a cholesterol/m β CD complex (Sigma, UK) at 37 °C for 2 hr during fura-2 loading and washing. Working concentrations were 1 mmole/L cholesterol plus 5 mmole/L m β CD or 0.5 mmole/L cholesterol plus 2.5 mmole/L m β CD. Cells were washed thoroughly with SBS before recordings to avoid the possibility that m β CD might chelate the TRPM3 agonist. For the generation of foam cells, VSMC were plated onto coverslips and incubated with media containing 0.5 mmole/L cholesterol plus 2.5 mmole/L m β CD and 2 % bovine serum albumin for 0-72 hr. To determine cholesterol uptake, cells were washed with 60 % isopropanol before the addition of Oil Red O. Cells were washed with water before stain was extracted by 100 % isopropanol. The optical density of the resulting solution was determined using a spectrophotometer at 500 nm. For Ca^{2+} imaging, cells were cholesterol loaded for 48 hr and washed thoroughly with SBS before use.

Wire myography

Vessels were mounted on two 40- μm diameter wires for isometric tension recording in a 410A dual wire myograph system (Danish Myo Technology, Denmark). The wires were separated by 1 mm to provide basal tension and the bath solution was at 37 °C gassed continuously with 95 % O_2 and 5 % CO_2 . The bath solution contained (mmole/L): 125 NaCl, 3.8 KCl, 25 NaHCO_3 , 1.5 MgSO_4 , 1.2 KH_2PO_4 , 8 D-glucose, 1.2 CaCl_2 , 0.02 EDTA.

Patch-clamp on proliferating VSMCs

Recordings were made using a planar patch-clamp system (Nanion, Germany) in whole-cell mode⁴. Prior to recordings, cells were detached from culture flasks with 0.05 % trypsin/EDTA and resuspended at a density of 1×10^6 – 5×10^7 per ml. The bath (external) solution contained (mmole/L): 145 NaCl, 3 KCl, 10 CsCl, 2 CaCl_2 , 2 MgCl_2 , 10 HEPES and 10 D-glucose; titrated to pH 7.4 with NaOH. The patch pipette (intracellular) solution contained (mmole/L): 40 EGTA, 17 CaCl_2 , 2 MgCl_2 , 8 NaCl, 1 Na_2ATP , 10 HEPES, 66 L-glutamic acid, 66 CsOH, titrated to pH 7.2 with CsOH (calculated unbound Ca^{2+} , 100 nmole/L). Voltage ramps were applied from -100 mV to +100 mV for 1 s every 10 s from a holding potential of 0 mV. Currents were filtered at 1 kHz and sampled at 3 kHz. Recordings were at room temperature.

Patch-clamp on contractile VSMCs and HEK 293 cells transiently expressing mouse TRPM3

For isolation of fresh contractile VSMCs, aortae were flushed slowly with 0.3 % CHAPS in Hanks solution to remove endothelial cells and incubated in Hanks solution containing 0.5 mg/ml collagenase,

0.1 mg/ml protease, 0.13 mg/ml hyaluronidase and 475 Units elastase for 5 min at 37 °C. The adventitia was gently removed, followed by a second incubation in fresh enzyme mix for 30 min at 37 °C. Enzymes were removed and the tissue was incubated in fresh Hanks solution at room temperature for 30 min before being agitated with a modified Pasteur pipette. Myocytes were plated onto coverslips, stored at 4 °C and used within 8 hr. Myocyte or HEK 293 cell recordings were made at room temperature using conventional whole-cell recording. Signals were amplified and sampled using an Axopatch 200B amplifier and pCLAMP 8 software (Molecular Devices, USA). Signals were filtered at 1 kHz and sampled at 2 kHz. Patch pipettes had resistance of 3-5 MΩ. The bath solution contained (mmole/L): 145 NaCl, 3 KCl, 10 CsCl, 2 CaCl₂, 2 MgCl₂, 10 HEPES and 10 D-glucose; titrated to pH 7.4 with NaOH. The patch pipette solution contained (mmole/L): 5 EGTA, 2 MgCl₂, 5 NaCl, 130 KCl, 3 Na₂ATP, 10 HEPES, titrated to pH 7.4 with KOH.

Secretion

IL-6 concentrations were quantified using a PeliKine-compact ELISA kit (Sanquin, Netherlands). MMP-9 was measured using a Quantikine ELISA Kit (R&D Systems, UK). Hyaluronan concentrations were quantified using a Corgenix ELISA kit (USA). Extracellular medium contained TPA (100 nmole/L) to induce tonic submaximal secretion.

Antibodies and labeling

Rabbit polyclonal anti-TRPM3 (TM3E3) and anti-TRPC1 (T1E3) antibodies have been described^{2,5}. For control experiments TM3E3 antibody was preadsorbed to 10 μM antigenic peptide (ratio 1:1) overnight at 4 °C prior to experiments (+pep). Antibody labeling of cells and intact vein sections was as described¹ except fixation of cells was for 4 min in 3 % paraformaldehyde and incubation with primary antibody was overnight at 4 °C. Tissue samples were incubated with TM3N1 anti-TRPM3 antibody targeted to the peptide CQEKEAEEPEKPTKE⁶ (1:400 dilution) or TM3E3 (1:2000 dilution) overnight at 4 °C. Images were collected using a laser confocal microscope (Zeiss, Germany) and analysed using Image J software (NIH, USA). For calcium imaging, cells were pre-incubated with TM3E3 or preimmune control antisera from the same rabbit at 1:500 dilution in DMEM media and standard bath solution for 3.5 hours at 37 °C. For contraction studies mouse aorta was pre-incubated with TM3E3 at 1:200 dilution or boiled control in Hanks solution overnight at 4 °C prior to recordings.

Data analysis

Averaged data are presented as mean±s.e.mean. Data produced in pairs (test and control) were compared using *t* tests, where statistical significance is indicated by * (P<0.05) and no significant difference by NS. When there were more than two groups, data sets were first compared using ANOVA. The *n* is the number of independent experiments, and *N* is the total number of individual cells, or wells of the 96-well plate. For experiments on saphenous vein, independent experiments were repeated on tissue/cells from at least 3 different patients.

Supplementary Results

There has been concern about whether sphingosine is indeed a TRPM3 activator, based on studies of mouse TRPM3³. While we observe stimulation of human TRPM3 by sphingosine, we also find that sphingosine inhibits action of TRPM3 by pregnenolone sulphate (Supplementary Fig VI). Our data support the concept of sphingosine as a modulator of TRPM3 but suggest that the polarity of the effect varies depending on the experimental design.

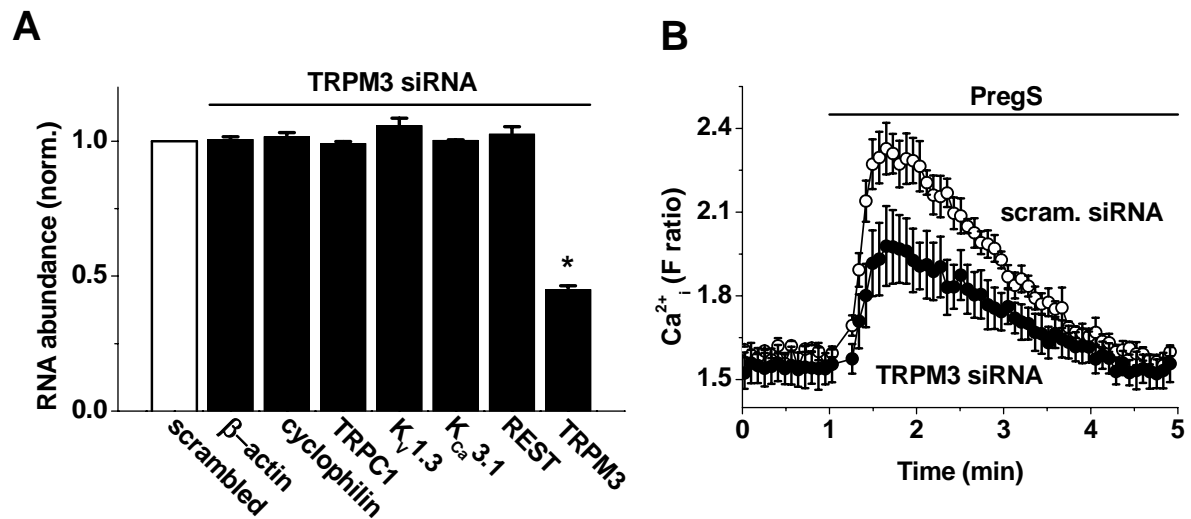
Supplementary References

1. Kumar B, Dreja K, Shah SS, Cheong A, Xu SZ, Sukumar P, Naylor J, Forte A, Cipollaro M, McHugh D, Kingston PA, Heagerty AM, Munsch CM, Bergdahl A, Hultgardh-Nilsson A, Gomez

- MF, Porter KE, Hellstrand P & Beech DJ. Upregulated TRPC1 channel in vascular injury in vivo and its role in human neointimal hyperplasia. *Circ Res*. 2006;98:557-563.
2. Naylor J, Milligan CJ, Zeng F, Jones C & Beech DJ. Production of a specific extracellular inhibitor of TRPM3 channels. *Br J Pharmacol*. 2008;155:567-573.
 3. Wagner TF, Loch S, Lambert S, Straub I, Mannebach S, Mathar I, Dufer M, Lis A, Flockerzi V, Philipp SE & Oberwinkler J. Transient receptor potential M3 channels are ionotropic steroid receptors in pancreatic beta cells. *Nat Cell Biol*. 2008;10:1421-1430.
 4. Milligan CJ, Li J, Sukumar P, Majeed Y, Dallas ML, English A, Emery P, Porter KE, Smith AM, McFadzean I, Beccano-Kelly D, Bahnasi Y, Cheong A, Naylor J, Zeng F, Liu X, Gamper N, Jiang LH, Pearson HA, Peers C, Robertson B & Beech DJ. Robotic multiwell planar patch-clamp for native and primary mammalian cells. *Nat Protoc*. 2009;4:244-255.
 5. Li J, Sukumar P, Milligan CJ, Kumar B, Ma ZY, Munsch CM, Jiang LH, Porter KE & Beech DJ. Interactions, functions, and independence of plasma membrane STIM1 and TRPC1 in vascular smooth muscle cells. *Circ Res*. 2008;103:e97-104.
 6. Grimm C, Kraft R, Sauerbruch S, Schultz G & Harteneck C. Molecular and functional characterization of the melastatin-related cation channel TRPM3. *J Biol Chem*. 2003;278:21493-21501.

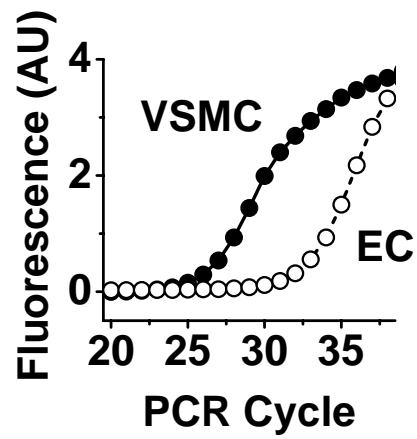
Supplementary Table I. Primers are for human sequences unless indicated.

mRNA target indicated by encoded protein	Primer (5'-3'; F, forward; R, reverse)	Predicted amplicon (bp)
TRPM3	F AGCAGTTCTACCTAACGT R CTTGCTCGACTAGACTTG	268
TRPM3 ₁₃₂₅ (i)	F CCTGGTGGAAATTTGGAAG R GAGTTGAGTGTGTTTGCT	335
TRPM3f (ii)	F GGAGCAGAGGTGAAACT R CCAAAGGCCAGGATGTC	215 (- insert) 290 (+ insert)
Mouse TRPM3	F ACCCCGTCAAGTAGTG R CCCCAAAGTTGGCGTA	295
β-actin	F TCGAGCAAGAGATGGC R TGAAGGTAGTTTCGTTGGATG	194
TRPC1	F TTAGCGCATGTGGCAA R CCACTTACTGAGGCTACTAAT	303
K _{Ca} 3.1	F CCGCCACTGGTTCGTGGCCA R CCATAGCCAATGGTCAGGAA	192
K _V 1.3	F GCTGGGATTGCTCATCTTCT R TGCTGCTGAAACCTGAAGTG	101
REST	F ACTTTGTCCTTACTCAAGTTCTCAG R ATGGCGGGTTACTTCATGTT	130
cyclophilin	F ACCCCACCGTGTTCCTTCGAC R TGGACTTGCCACCAGTGCCA	292



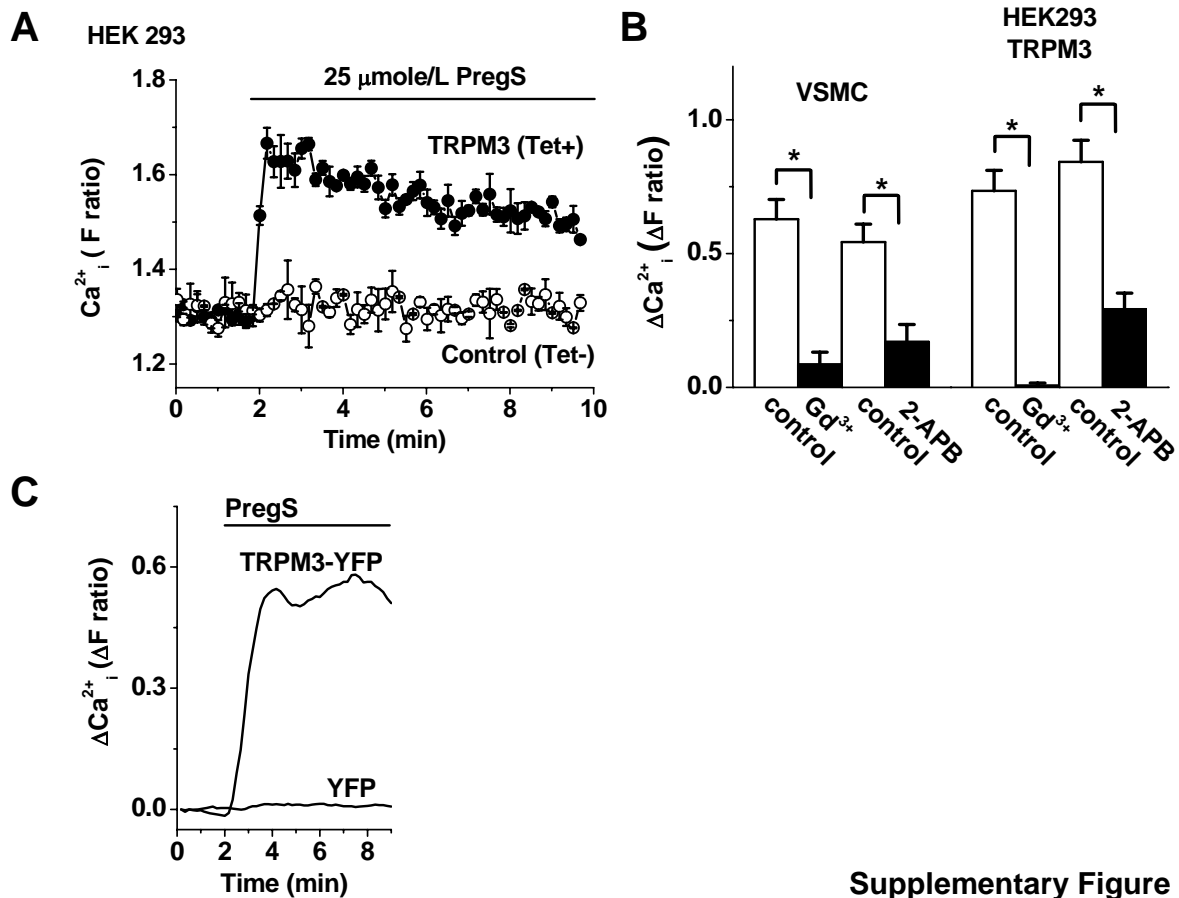
Supplementary Figure I

Supplementary Figure I. Specificity and validation of TRPM3 knock-down by RNAi. (A) Summary of real-time quantitative RT-PCR analysis to determine the abundance of mRNAs encoding the indicated proteins in human VSMCs. Each mRNA was quantified in paired experiments comparing cells transfected with TRPM3 siRNA or scrambled (control) siRNA. The abundance of each mRNA in the TRPM3 siRNA group was normalized to that in its own control group. The data show that TRPM3 mRNA was reduced in abundance by TRPM3 siRNA and that other mRNAs were not affected ($n=3$). (B) Effect of Smart pool TRPM3 siRNA-2 on the intracellular Ca^{2+} response to 100 μ mol/L PregS ($N=4$ for each).



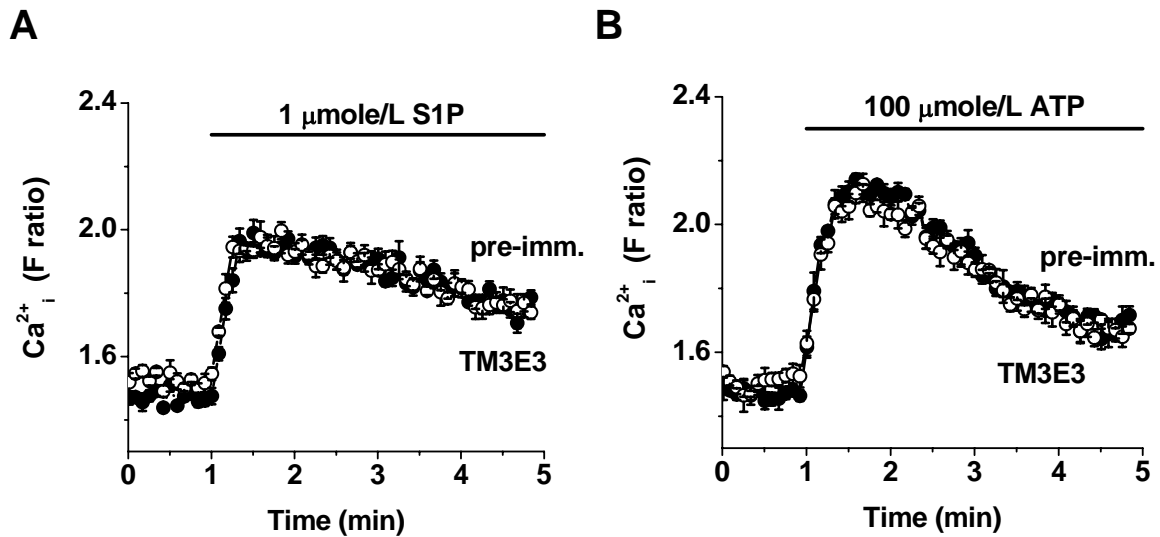
Supplementary Figure II

Supplementary Figure II. Real-time RT-PCR comparison of TRPM3 mRNA abundance in cultured human saphenous vein vascular smooth muscle cells (VSMCs) and endothelial cells (ECs).



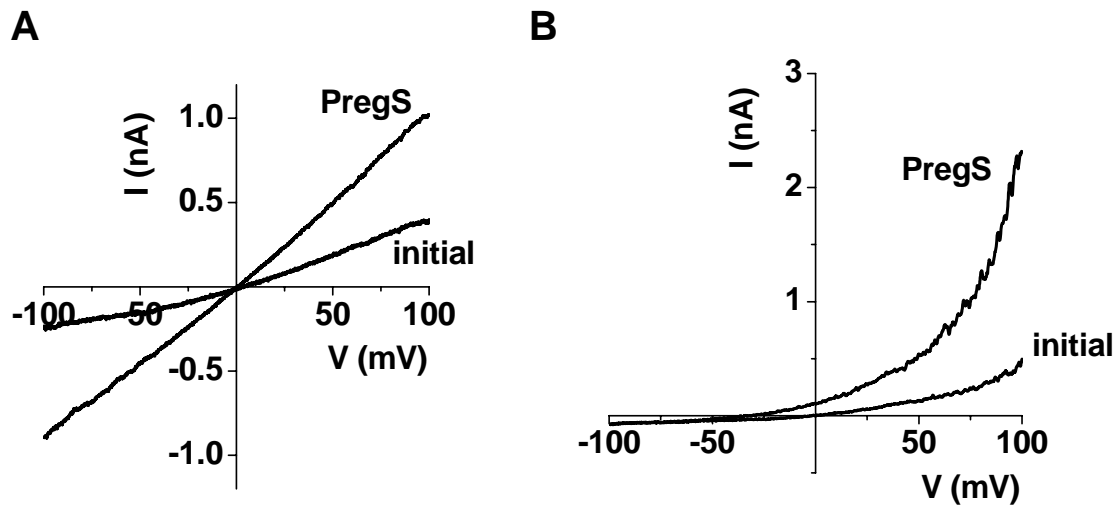
Supplementary Figure III

Supplementary Figure III. Effects of chemical agents on PregS responses. The data are from intracellular Ca^{2+} measurements. (A) Example comparison of responses to 25 $\mu\text{mole/L}$ PregS in HEK 293 cells induced (Tet+) or not induced (Tet-) to express exogenous human TRPM3. (B) Mean data for amplitudes of responses to 25 $\mu\text{mole/L}$ PregS without (control) or with the presence of 0.1 mmole/L gadolinium ions (Gd^{3+}) or 75 $\mu\text{mole/L}$ 2-aminoethoxydiphenylborate (2-APB) ($n/N = 7/23$ and $3/28$ respectively). DMSO (dimethylsulphoxide) was the solvent and control for 2-APB. Responses are compared for HEK 293 cells expressing exogenous TRPM3 and human VSMCs. (C) Typical microscope-based Ca^{2+} measurement data showing responses to 25 $\mu\text{mole/L}$ PregS in wild-type HEK 293 cells transiently expressing YFP-tagged human TRPM3 or YFP only (representative of $n=3$ and $N=27-48$).



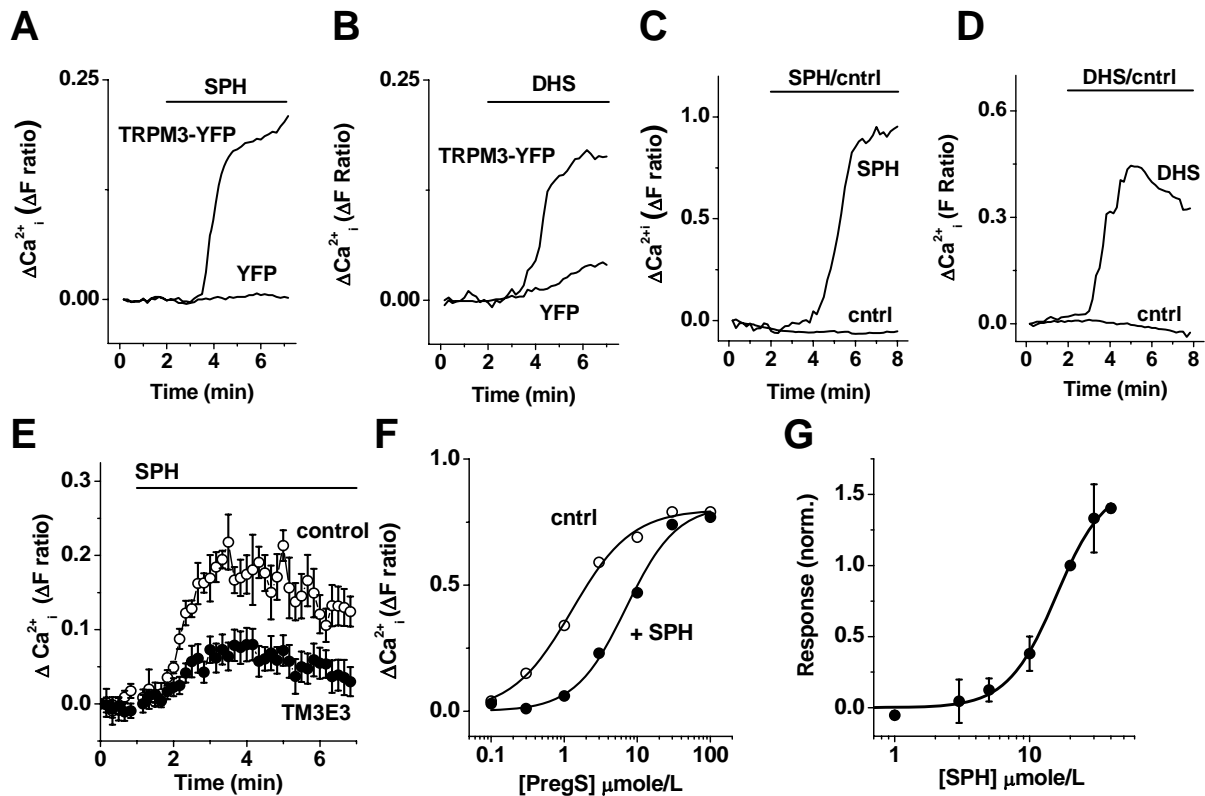
Supplementary Figure IV

Supplementary Figure IV. Functional specificity of anti-TRPM3 antibody TM3E3. The data show example intracellular Ca²⁺ measurements from human VSMCs. Cells were exposed to extracellular 1 $\mu\text{mole/L}$ sphingosine-1-phosphate (S1P, A) or 100 $\mu\text{mole/L}$ adenosine 5'-triphosphate (ATP, B). The responses were at least partly due to intracellular Ca²⁺-release following activation of G-protein coupled receptors. Incubation with TM3E3 had no effect compared with the preimmune serum control ($n/N = 3/17$ and $4/22$).



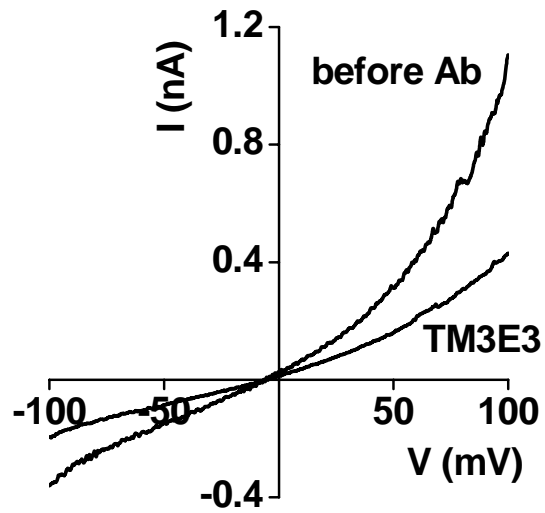
Supplementary Figure V

Supplementary Figure V. Current-voltage relationships (I-Vs) for PregS-induced currents in human VSMCs. The I-Vs marked 'initial' were obtained before bath-application of 25 μ mole/L PregS. (A) Typical I-Vs observed in 27 out of 37 recordings. (B) Typical I-Vs observed in 10 out of 37 recordings.



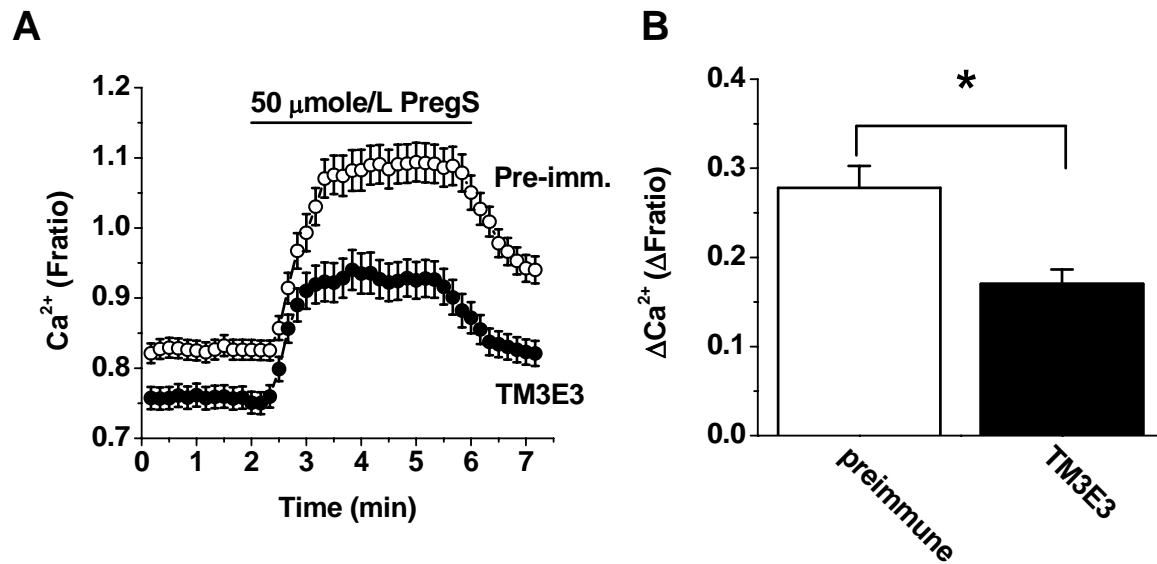
Supplementary Figure VI

Supplementary Figure VI. Effects of sphingosine or dihydrosphingosine. Data are from intracellular Ca^{2+} measurements from HEK 293 cells (A, B, F) or VSMCs (C, D, E, G). Cells were exposed to 20 $\mu\text{mole/L}$ sphingosine (SPH) or dihydrosphingosine (DHS), ethanol vehicle control (cntrl), or the concentrations of pregnenolone sulphate (PregS) indicated in (F). (A, B) Typical data from HEK 293 cells transiently expressing YFP-tagged human TRPM3 or YFP only (representative of $n=3-6$ and $N=9-29$). (D, E) Typical data from VSMCs (representative of $n=3-6$ and $N=9-29$). (E) Example responses to 20 $\mu\text{mole/L}$ SPH after pretreatment with TM3E3 antiserum or its preimmune control. (F) Representative experiment for the concentration-dependence of PregS responses in the absence (cntrl) or presence (+SPH) of 20 $\mu\text{mole/L}$ sphingosine ($N=2$, representative of $n=3$). HEK 293 cells were induced to express exogenous human TRPM3 (Tet+). (G) Concentration-dependence of Ca^{2+} responses to sphingosine (SPH) in VSMCs normalized to responses to 20 $\mu\text{mole/L}$ SPH ($n/N=4/24$). (F, G) Fitted curves are Hill equations.



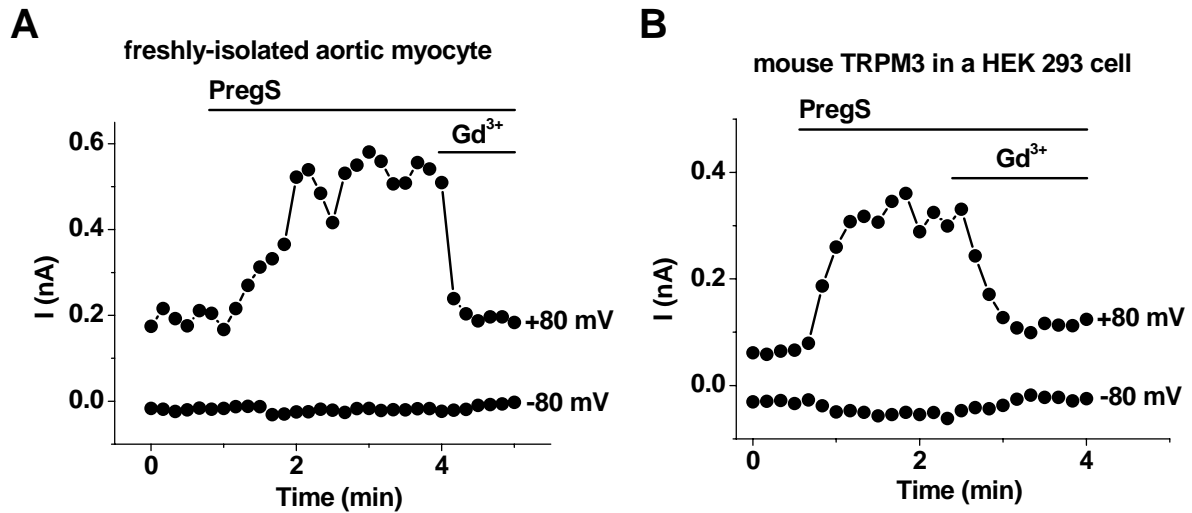
Supplementary Figure VII

Supplementary Figure VII. Typical current-voltage relationship (I-Vs) for constitutive membrane current in a human VSMC, showing the effect of TM3E3 anti-TRPM3 blocking antibody (example from $n=8$).



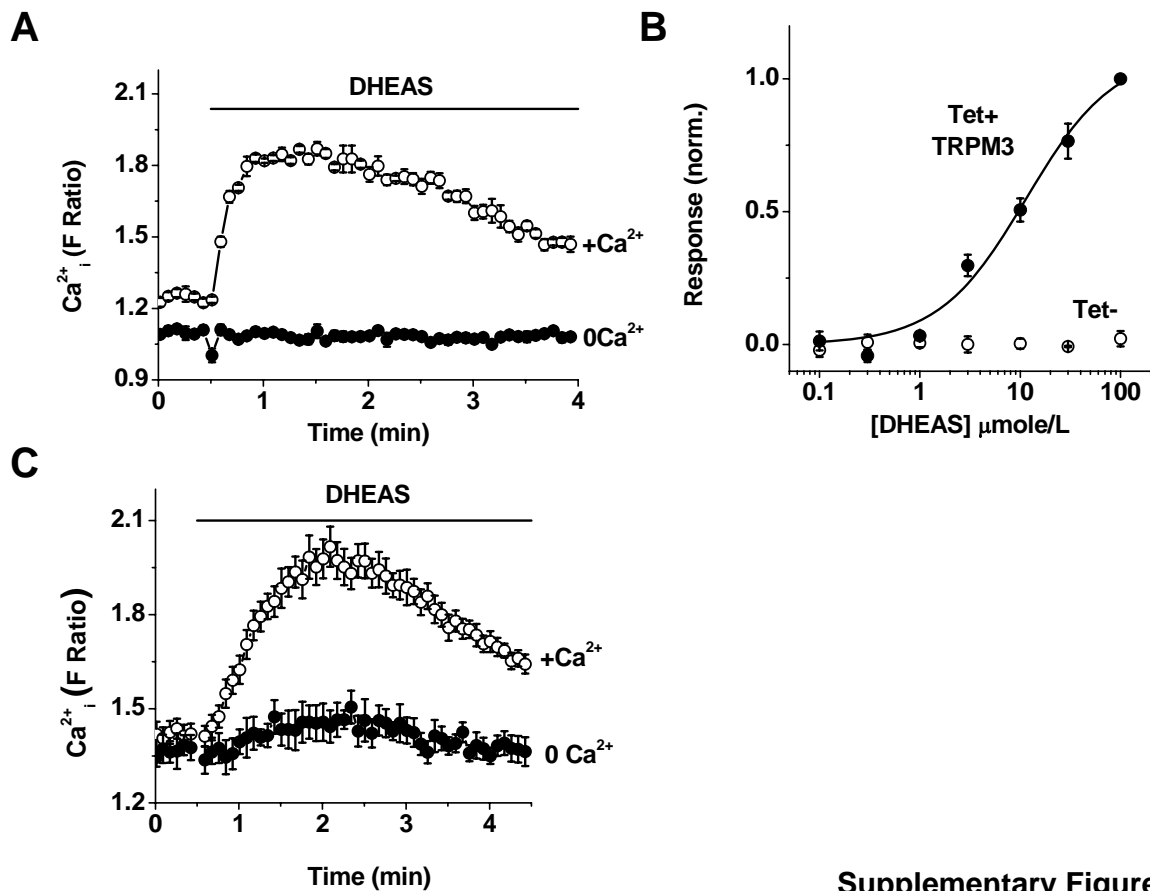
Supplementary Figure VIII

Supplementary Figure VIII. Inhibition of murine TRPM3 by anti-TRPM3 blocking antibody (TM3E3). The data are from intracellular Ca²⁺ measurements performed on HEK 293 cells transiently transfected with mouse TRPM3 α 2. (A) Mean time-series data for experiments comparing the 50 $\mu\text{mole/L}$ PregS response in cells preincubated in TM3E3 or its preimmune control ($n/N = 6/66$ and $6/64$). Suppression of the basal Ca²⁺ signal and the PregS response are evident. (B) As for (A) but comparing only the amplitudes of the PregS responses.



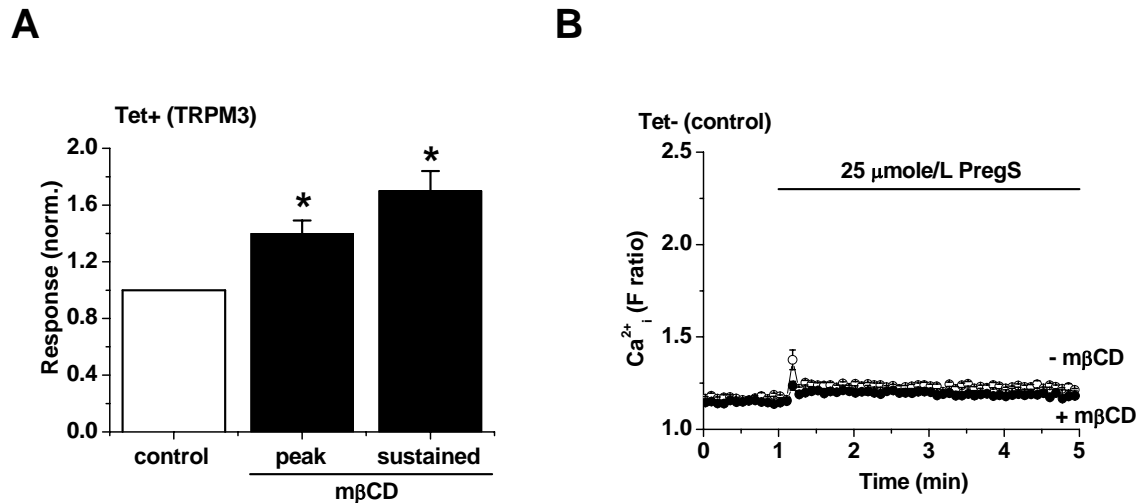
Supplementary Figure IX

Supplementary Figure IX. Pregnenolone sulphate responses in smooth muscle cells freshly-isolated from the mouse aorta compared with HEK 293 cells over-expressing mouse TRPM3. (A) From 5 independent recordings, example ionic currents recorded at +80 and -80 mV from a freshly isolated mouse aorta smooth muscle cell. (B) From 15 independent recordings, example ionic currents recorded at +80 and -80 mV from a HEK 293 cell heterologously expressing mouse TRPM3. Pregnenolone sulphate (PregS, 100 μ mole/L) and gadolinium (Gd^{3+} , 100 μ mole/L) were bath-applied as indicated by horizontal bars. HEK 293 cells not transfected with TRPM3 failed to respond to pregnenolone sulphate ($n=13$).



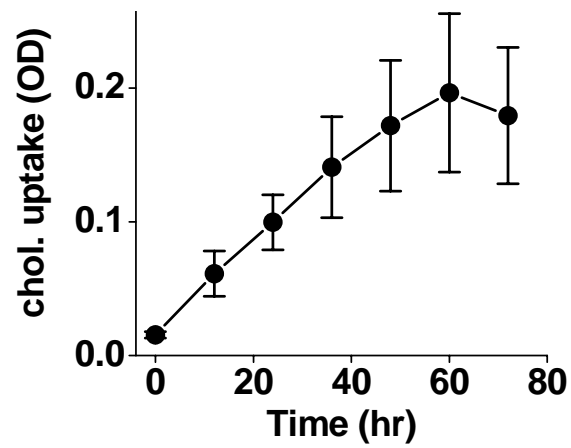
Supplementary Figure X

Supplementary Figure X. Stimulation by dihydroepiandrosterone sulphate (DHEAS). (A, B) The data show intracellular Ca²⁺ measurement experiments from HEK 293 cells induced to express exogenous human TRPM3 (Tet+) or not (Tet-). (A) In Tet+ cells, a typical paired comparison showing Ca²⁺ responses to 30 µmole/L DHEAS in the presence and absence of extracellular 1.5 mmole/L Ca²⁺ ($N=4$ for each condition; representative of $n=4$). (B) Concentration-dependence of Ca²⁺ responses to DHEAS, comparing mean data for Tet+ and Tet- cells ($n/N=3/9$ for each; estimated EC_{50} for Tet+ cells 11.5 µmole/L). Tet+ cell data are the same as shown in Fig. 5B of the main paper. (C) In VSMCs, a typical paired comparison showing Ca²⁺ responses to 100 µmole/L DHEAS in the presence and absence of extracellular 1.5 mmole/L Ca²⁺ ($N=4$ for each condition; representative of $n=4$).



Supplementary Figure XI

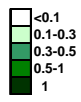
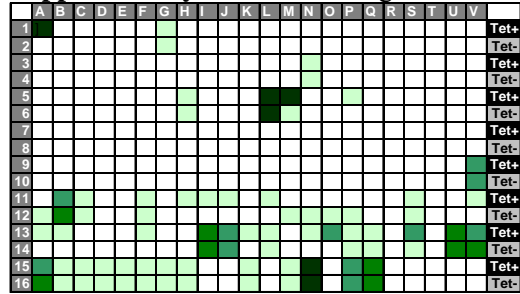
Supplementary Figure XI. Stimulation of TRPM3 by methyl- β -cyclodextrin (m β CD). (A) HEK 293 cells were induced to express exogenous human TRPM3 (Tet+). The data summarise paired comparisons of peak and sustained responses to 25 μ mole/L PregS in cells pre-incubated for 1 hr with 2.78 mmole/L m β CD or without m β CD ($N = 8$ for each condition). (B) Typical paired experiment showing lack of effect of 25 μ mole/L PregS or 2.78 mmole/L m β CD in non-induced HEK 293 cells (Tet-) ($N=8$).



Supplementary Figure XII

Supplementary Figure XII. Time course for cholesterol uptake by VSMCs during loading with exogenous cholesterol (0.5 mmole/L) and measured by the optical density (OD) of Oil Red O.

Supplementary File I. Decoding of the chemical screen.



Chemical	Chemical	Chemical	Chemical						
PregS	A1	1	A2	0.021	Cholesterol	U7	0.058	U8	0.082
Vehicle (DMSO)	B1	0.018	B2	0.019	Dihydroliipoic acid	V7	0.057	V8	0.058
AM 92016	C1	0.045	C2	0.032	Oleic acid	A9	0.08	A10	0.073
Amiloride hydrochloride	D1	0.041	D2	0.045	Linoleic acid	B9	0.062	B10	0.094
4-Aminopyridine	E1	0.028	E2	0.038	PIP2	C9	0.065	C10	0.08
Amiodarone hydrochloride	F1	0.021	F2	0.023	Lipase	D9	0.086	D10	0.092
2-Aminoethyl diphenylborinate	G1	0.085	G2	0.096	Cholesterol esterase	E9	0.087	E10	0.093
Amriptyline hydrochloride	H1	0.031	H2	0.024	Sphingosine	F9	0.051	F10	0.036
Anandamide	I1	0.03	I2	0.036	DHS	G9	0.039	G10	0.016
Antazoline hydrochloride	J1	0.029	J2	0.035	Safingol	H9	0.053	H10	0.029
Benzocaine	K1	0.03	K2	0.021	Sphingomyelin	I9	0.018	I10	0.02
Bepiridil hydrochloride	L1	0.035	L2	0.019	SPC	J9	0.023	J10	0.036
Bisindolylmaleimide I	M1	0.036	M2	0.032	LPC (egg yolk)	K9	0.036	K10	0.025
Bupivacaine	N1	0.034	N2	0.035	ET-18-OCH3	L9	0.05	L10	0.017
Calmidazolium chloride	O1	0.015	O2	0.075	Methanandamide	M9	0.029	M10	0.013
Canrenic acid potassium salt	P1	0.016	P2	0.017	Stearic acid	N9	0.031	N10	0.023
Carbamazepine	Q1	0.013	Q2	0.015	α-lipoic acid	O9	0.023	O10	0.009
Chloroquine diphosphate	R1	0.01	R2	0.013	Palmitic acid	P9	0.041	P10	0.016
(+)-Chlorpheniramine maleate	S1	0.013	S2	0.012	Carbacyclin	Q9	0.078	Q10	0.043
Chlorpromazine hydrochloride	T1	0.021	T2	0.019	Angiotensin II	R9	0.054	R10	0.075
Chromanol	U1	0.015	U2	0.017	Endomorphin I	S9	0.064	S10	0.077
Citalopram hydrobromide	V1	0.03	V2	0.043	LHRH	T9	0.058	T10	0.074
Clotrimazole	A3	0.024	A4	0.031	Melanin Conc. Hormone	U9	0.065	U10	0.071
CP 339818 HCl	B3	0.023	B4	0.021	Bradykinin	V9	0.383	V10	0.49
Dexamethasone	C3	0.016	C4	0.013	Substance P fragment	A11	0.067	A12	0.21
DIDS	D3	0.015	D4	0.012	Arg Vasopressin	B11	0.433	B12	0.748
5,5-Diphenylhydantoin	E3	0.034	E4	0.027	Arg Vasostocin	C11	0.187	C12	0.226
Diltiazem HCl	F3	0.04	F4	0.034	Oxytocin	D11	0.09	D12	0.069
Diphenhydramine HCl	G3	0.022	G4	0.022	Thyrotropin RH	E11	0.08	E12	0.073
Doxepin HCl	H3	0.025	H4	0.03	Neurotensin	F11	0.167	F12	0.13
Epigallocatechin-3-gallate	I3	0.025	I4	0.035	Bombesin	G11	0.089	G12	0.076
Erythromycin	J3	0.022	J4	0.026	Leukotriene B4	H11	0.079	H12	0.108
Ethosuximide	K3	0.027	K4	0.027	Leukotriene C4	I11	0.083	I12	0.099
Felodipine	L3	0.033	L4	0.023	Leukotriene D4	J11	0.081	J12	0.108
Flecainide acetate	M3	0.033	M4	0.031	Leukotriene E4	K11	0.067	K12	0.09
Fluoxetine HCL	N3	0.101	N4	0.089	Prostaglandin H2	L11	0.105	L12	0.071
Fluspirilene	O3	0.04	O4	0.024	REV 5901	M11	0.077	M12	0.149
Fluvoxamine maleate	P3	0.037	P4	0.034	Prostaglandin A2	N11	0.082	N12	0.174
Gabapentin	Q3	0.017	Q4	0.018	Prostaglandin B2	O11	0.082	O12	0.115
Haloperidol	R3	0.024	R4	0.015	Prostaglandin D2	P11	0.095	P12	0.101
Impipamine HCl	S3	0.011	S4	0.016	Prostaglandin E1	Q11	0.091	Q12	0.065
Indapamide	T3	0.017	T4	0.019	Prostaglandin E2	R11	0.082	R12	0.079
Capsaicin	U3	0.043	U4	0.034	Prostaglandin F2a	S11	0.107	S12	0.095
Ketoconazole	V3	0.02	V4	0.026	Carbocyclic thromboxane A2	T11	0.071	T12	0.179
Lamotrigine	A5	0.019	A6	0.026	Thromboxane B2	U11	0.08	U12	0.04
Lidocaine	B5	0.02	B6	0.028	U-46619	V11	0.106	V12	0.05
Linopirdine	C5	0.029	C6	0.019	AH6809	A13	0.111	A14	0.064
Loperamide HCl	D5	0.077	D6	0.073	Carbaprostacyclin	B13	0.12	B14	0.067
Mepivacaine	E5	0.022	E6	0.017	Sulprostone	C13	0.076	C14	0.06
(+)-Methoxyverapamil HCl	F5	0.033	F6	0.035	BW245C	D13	0.093	D14	0.055
Mexiletene HCl	G5	0.018	G6	0.022	trans-BTP Dioxolane	E13	0.054	E14	0.065
Mibefradil diHCl	H5	0.065	H6	0.128	Prostaglandin I2	F13	0.099	F14	0.074
W-7	I5	0.047	I6	0.048	15d-PGJ2	G13	0.084	G14	0.074
N-acetylprocainamide HCl	J5	0.019	J6	0.021	Prostaglandin K1	H13	0.067	H14	0.085
Nicardipine HCl	K5	0.026	K6	0.028	L-α-phosphatidic acid	I13	0.59	I14	0.608
Nicotine	L5	1.508	L6	1.334	S-1-P	J13	0.4	J14	0.3
Nifedipine	M5	1.005	M6	0.276	C2 ceramide	K13	0.097	K14	0.071
Niflumic acid	N5	0.045	N6	0.081	C8 ceramide	L13	0.135	L14	0.104
Nimodipine	O5	0.021	O6	0.03	C8 ceramide-1P	M13	0.081	M14	0.082
Nisoldipine	P5	0.22	P6	0.084	Arachadonic acid	N13	0.15	N14	0.074
Nitrendipine	Q5	0.064	Q6	0.061	Hepoxilin A3	O13	0.348	O14	0.079
Nortryptlyline	R5	0.039	R6	0.041	REV 5901 para isomer	P13	0.15	P14	0.115
Papaverine HCl	S5	0.027	S6	0.043	Misoprostol	Q13	0.132	Q14	0.11
Perhexiline maleate	T5	0.066	T6	0.085	SPC	R13	0.08	R14	0.09
3-phenyl-1-pyrrolidin-1-yl-propenone	U5	0.037	U6	0.048	B-cyclodextrin	S13	0.302	S14	0.141
Procainamide	V5	0.03	V6	0.029	Ginkgolide A	T13	0.088	T14	0.09
Propafenone HCl	A7	0.022	A8	0.027	PAF-16	U13	0.535	U14	0.494
Quinidine sulfate	B7	0.034	B8	0.053	PAF-16 antagonist	V13	0.386	V14	0.498
QX222	C7	0.043	C8	0.046	lyso PAF-16	A15	0.437	A16	0.701
QX314	D7	0.028	D8	0.036	PAF-18	B15	0.305	B16	0.225
R(+)-SCH-23390 HCL	E7	0.028	E8	0.038	lyso PAF-18	C15	0.299	C16	0.225
RCL R41,038-1	F7	0.026	F8	0.037	5(S),6(R)-DIHETE	D15	0.237	D16	0.143
Riluzole	G7	0.046	G8	0.055	5(S),15(S)-DIHETE	E15	0.246	E16	0.181
Ruthenium red	H7	0.048	H8	0.055	8(S),15(S)-DIHETE	F15	0.246	F16	0.232
SKF 96365	I7	0.019	I8	0.023	12(R)-DIHETE	G15	0.258	G16	0.224
(+)-Solatol HCl	J7	0.021	J8	0.015	15(S)-DIHETE	H15	0.258	H16	0.204
Spiroonactone	K7	0.025	K8	0.02	7-ketocholesterol	I15	0.013	I16	0.003
SR 33805	L7	0.019	L8	0.024	7 B-hydroxy cholesterol	J15	0.025	J16	0.003
(+)-Sulpiride	M7	0.018	M8	0.018	bovine SPH	K15	0.15	K16	0.25
TEA Cl	N7	0.017	N8	0.039	Palmitoyl CoA	L15	0.025	L16	0.025
Thionidazine HCl	O7	0.093	O8	0.084	4aPDD	M15	0.22	M16	0.2
Tocainide	P7	0.028	P8	0.025	LPI	N15	1.2	N16	1
Triamterene	Q3	0.021	Q4	0.019	Gd	O15	0.07	O16	0.09
Venlafaxine	R7	0.018	R8	0.017	CCh	P15	0.49	P16	0.43
Verapamil	S7	0.021	S8	0.02	H2O2	Q15	0.6	Q16	0.7
Vinpocetine	T7	0.023	T8	0.039	progesterone	R15	0.003	R16	0.003
					5βpreg3a	S15	0.003	S16	0.003
					5αpreg3a	T15	0.003	T16	0.003
					5preg3B	U15	0.003	U16	0.003
					3B-OH-3a	V15	0.003	V16	0.003